Eur. Phys. J. C (2008) 56: 511–528
DOI 10.1140/epjc/s10052-008-0672-9

THE EUROPEAN PHYSICAL JOURNAL C

Regular Article - Theoretical Physics

Heavy-flavor tagging and the supersymmetry reach of the CERN Large Hadron Collider

R.H.K. Kadala[1,2,a], **P.G. Mercadante**[3,b], **J.K. Mizukoshi**[4,c], **Xerxes Tata**[2,d]

[1]College of Natural Sciences, Hawaii Pacific University, Kaneohe, HI 96744, USA
[2]Department of Physics and Astronomy, University of Hawaii, Honolulu, HI 96822, USA
[3]Instituto de Física Teórica, Universidade Estadual Paulista, São Paulo, SP, Brazil
[4]Centro de Ciências Naturais e Humanas, Universidade Federal do ABC, Santo André, SP, Brazil

Received: 30 May 2008 / Published online: 6 August 2008
© Springer-Verlag / Società Italiana di Fisica 2008

Abstract The branching fraction for the decays of gluinos to third generation quarks is expected to be enhanced in classes of supersymmetric models where either third generation squarks are lighter than other squarks, or in mixed-higgsino dark matter models constructed so as to be in concordance with the measured density of cold dark matter. In such scenarios, gluino production events at the CERN Large Hadron Collider should be rich in top and bottom quark jets. Requiring b jets in addition to $E_T^{\rm miss}$ should, therefore, enhance the supersymmetry signal relative to Standard Model backgrounds from V + jet, VV and QCD backgrounds ($V = W, Z$). We quantify the increase in the supersymmetry reach of the LHC from b-tagging in a variety of well-motivated models of supersymmetry. We also explore "top tagging" at the LHC. We find that while the efficiency for this turns out to be too low to give an increase in reach beyond that obtained via b-tagging, top tagging can indeed provide a confirmatory signal if gluinos are not too heavy. We also examine c jet tagging but find that it is not useful at the LHC. Finally, we explore the prospects for detecting the direct production of third generation squarks in models with an inverted squark mass hierarchy. This is signaled by b jets + $E_T^{\rm miss}$ events being harder than in the Standard Model, but softer than those from the production of gluinos and heavier squarks. We find that while these events can be readily separated from the SM background (for third generation squark masses ∼300–500 GeV), the contamination from the much heavier gluinos and squarks remains formidable if these are also accessible.

[a] e-mail: kadala@phys.hawaii.edu
[b] e-mail: mercadan@fnal.gov
[c] e-mail: mizuka@ufabc.edu.br
[d] e-mail: tata@phys.hawaii.edu

1 Introduction

Weak scale supersymmetry (SUSY) [1–4] is the best motivated and most carefully studied extension of the Standard Model (SM). The hypothesis of TeV scale superpartners of SM particles simultaneously stabilizes the gauge hierarchy, accounts for gauge coupling unification, and naturally accommodates the measured relic density in the minimal extension of the SM. This is especially exciting because squarks and gluinos will be produced at observable rates at the Large Hadron Collider (LHC) if their masses are smaller than 2–3 TeV [5–13]. Supersymmetric models generically allow for renormalizable baryon- and lepton-number violating operators that lead to proton decay at the typical weak interaction rate, and they would be strongly excluded unless there is an additional symmetry that forbids these interactions. Assuming that R-parity serves this purpose, heavy superpartners must decay into lighter sparticles until the decay terminates in the lightest supersymmetric particle (LSP), which must be stable. Cosmological considerations require that the LSP is electrically and color neutral so that it escapes the experimental apparatus without significant deposition of energy. Then, superpartner production at colliders is generically signaled by multi-jet plus multi-lepton events with large amounts of $E_T^{\rm miss}$ carried off by the escaping LSPs. We will assume that the lightest neutralino is the LSP as is the case in many models.

Remarkably, weak scale SUSY models with a stable neutralino LSP naturally lead to the right magnitude for the measured relic density of thermally produced cold dark matter [14],

$$\Omega_{\rm CDM}h^2 = 0.111^{+0.011}_{-0.015} \quad (2\sigma), \tag{1}$$

if superpartner masses are ∼100 GeV. Assuming thermal production and standard Big Bang cosmology, the upper

limit from (1) provides a stringent constraint on any theory with stable weakly interacting particles, in particular on weak scale SUSY theories. Since dark matter may well consist of several components, the contribution from any single component may well be insufficient to saturate the observed value, so that strictly speaking the relic density measurement serves as an upper bound,

$$\Omega_{\widetilde{Z}_1} h^2 < 0.12, \tag{2}$$

on the relic density of neutralinos, or, for that matter, on the density of any other stable particle.

Direct searches for charged sparticles at LEP 2 have resulted in lower limits of about 100 GeV on chargino and selectron masses, and slightly lower limits on the masses of smuons and staus [15]. Since neutralinos can annihilate via t-channel sfermion exchange, the measured value of the relic density, on the other hand, favors sfermions lighter than about 100 GeV, resulting in some tension with the LEP 2 bounds. In many constrained models where all sparticle masses and couplings are fixed by just a few parameters, such light sparticles often also lead to measurable deviations in *other* observables and hence are disfavored. If the SUSY mass scale is raised to avoid these constraints, the annihilation cross section which is proportional to $\frac{1}{M^2_{\rm SUSY}}$ is correspondingly reduced, and the neutralino relic density turns out to be too large. One way to fix this is by invoking non-thermal relics or non-standard cosmology to dilute the relic density. However, it seems much more economical to invoke SUSY mechanisms that enhance the neutralino annihilation rate to bring their thermal relic density in line with (1).

The primary reason for the low neutralino annihilation rate lies in the fact that the LSP is dominantly a bino in many models with assumed gaugino mass unification, where the bino and wino masses are related by $M_1 \simeq \frac{1}{2} M_2$. The annihilation of bino pairs to gauge bosons is forbidden, because $SU(2) \times U(1)$ precludes the couplings of binos to the gaugino–gauge boson system, while annihilation to fermions may be suppressed by large sfermion masses and the relatively small hypercharge coupling. Finally, annihilation to Higgs boson pairs is suppressed by the (usually large) higgsino mass, as well as by the relatively small hypercharge gauge coupling. This suggests several ways in which the neutralino annihilation rate may be enhanced to bring their thermal relic density in accord with (1).

- We can arrange the mass of a charged or colored sparticle to be close to that of the LSP. Since these colored/charged sparticles can annihilate efficiently, interactions between them and the neutralino which maintain thermal equilibrium will necessarily also reduce the neutralino relic density [16–18]. Within the mSUGRA model, the co-annihilating sparticle is usually either the scalar tau [19–24] or the scalar top [25–27], but different choices are possible in other models.
- We can arrange $2m_{\widetilde{Z}_1} \simeq m_A \simeq m_H$, so that neutralino annihilation is resonantly enhanced through s-channel heavy Higgs boson exchange [28–35]. The large widths of A and H together with the thermal motion of the LSPs in the early universe then enhances the annihilation cross section over a considerable range of parameters. Within the mSUGRA model, this is possible only if $\tan\beta$ is very large. However, in models with non-universal Higgs mass (NUHM) parameters, where the Higgs scalar mass parameters do not unify with matter scalar parameters as in mSUGRA [36–45], agreement with (1) may be obtained via resonant A/H annihilation for any value of $\tan\beta$. We mention that resonantly enhanced annihilation may also occur via h exchange, albeit for a much smaller range of parameters [46, 47].
- It is also possible to obtain an enhanced neutralino annihilation rate if the light top squark, $\tilde{t}_1$, is relatively light, so that the neutralinos efficiently annihilate via $\widetilde{Z}_1\widetilde{Z}_1 \to t\bar{t}$ [48–50], or in NUHM models via $\widetilde{Z}_1\widetilde{Z}_1 \to u\bar{u}$ or $c\bar{c}$, via t-channel top- or right-squark exchanges, respectively [44, 45].

Instead of adjusting sparticle masses, we can also adjust the composition of the neutralino. More specifically, we have the following options.

- We can increase the higgsino content of the neutralino so that its coupling to electroweak gauge bosons is increased, leading to mixed-higgsino dark matter (MHDM). Within the mSUGRA framework, we can only do so in the so-called hyperbolic branch/focus point (HB/FP) region where m_0 takes on multi-TeV values [51–53], but in NUHM models this is possible for *all* values of m_0 [44, 45]. The higgsino content may also be increased by relaxing the assumed high scale universality between gaugino masses. The usually assumed universality of gaugino masses follows if the auxiliary field that breaks supersymmetry does not break the underlying grand unification symmetry; if this is not the case, non-universal gaugino masses may result. It has been shown that if the GUT scale gluino mass is smaller than the other gaugino masses, $m^2_{H_u}$ does not run as negative as usual, yielding a smaller value of μ^2, resulting in an increased higgsino content of $\widetilde{Z}_1$ [54–57]. This has been dubbed "low M_3 dark matter" (LM3DM). Very recently [58] it has been pointed out that increasing the GUT scale wino mass parameter from its unified value also results in a low value of $|\mu|$, resulting in consistency with (1) via MHDM.
- Finally, depending on the gauge transformation property of the SUSY breaking auxiliary field, it may also be possible to enhance the wino content of the neutralino leading to mixed wino dark matter (MWDM) [59–61]. This requires that the weak scale values of bino and wino masses to be approximately equal. If instead these are roughly

equal in magnitude but differ in sign, bino–wino mixing is suppressed, but agreement with the observed relic density is possible via bino–wino co-annihilation (BWCA) [62].

These various mechanisms result in characteristic modifications of supersymmetry signals at the LHC, at the proposed linear electron–positron collider (LC) or at experiments for direct and indirect detection of the relic neutralinos in our galactic halo [63]. Of interest to us here is the potential for an enhanced rate for bottom quark production in SUSY events that occurs for MHDM, as exemplified by (but not limited to) the HB/FP region of the mSUGRA model [64, 65], or models where third generation squarks are significantly lighter than other squarks as, for instance, in the stop co-annihilation region of mSUGRA, in so-called inverted hierarchy models in which third generation sfermions are much lighter than those of the first two generations [66–70], or in the framework suggested in Refs. [48–50].

We have multiple goals for this study. First, we follow up an earlier investigation [65] by three of us, where it was shown that using b jet tagging techniques that are available at the LHC, the SUSY reach may be enhanced by as much as 20% for parameters in the HB/FP of the mSUGRA model. Toward this end, we examine the reach of the LHC with and without b jet tagging, in several models motivated by the relic density measurement just discussed[1] as well as by other considerations. We find that the reach is increased by different amounts, and that sometimes requiring b-tagging even reduces the reach. One aim of this study is to precisely delineate the circumstances under which b jet tagging will significantly enhance the LHC reach. Second, since SUSY events are frequently also enriched in t jets, we examine prospects for top jet tagging in SUSY events at the LHC. Third, motivated by the fact that c-tagging has been suggested [71] as a way to enhance the t-squark SUSY signal at the Femilab Tevatron, we also examine whether tagging charm jets may serve to increase the SUSY reach of the LHC. Finally, since third generation squarks are expected to be lighter than other squarks in many models, we explore the prospects for using b-tagging to isolate signals from their direct production from SM backgrounds as well as from other sparticle production processes.

The rest of this paper is organized as follows. In Sect. 2 we introduce the various models that offer the potential for an enhanced b jet signal, and we discuss the parameter space for each of these models. In Sect. 3, we discuss our event simulation using ISAJET [72], and we see how we may use this to model the LHC environment. In Sect. 4 we examine a large set of selection cuts that may be used to optimize the SUSY signal and design a set of cuts that we believe should work for a wide class of models over their entire parameter range: we then use these to obtain projections for how b jet tagging would enhance the LHC reach for these models. We discuss the prospects for top tagging in Sect. 5. In Sect. 6, we describe our strategy for isolating the signal for the direct production of third generation squarks from SM backgrounds as well as from contamination from the production of gluinos and heavier squarks, since the observation of such a signal would unequivocally point to models with an inverted mass hierarchy. Finally, we report on our (negative) results for using charm tagging to enhance the SUSY signal at the LHC in Sect. 7. We summarize our findings in Sect. 8.

2 Models

In this section, we discuss several models in which we may expect third generation fermions to be preferentially produced in SUSY models. We begin with the familiar mSUGRA model and work our way through various other models, motivated either by the relic density observation discussed in Sect. 1 or by other considerations.

2.1 The mSUGRA model

The mSUGRA model [73–78], whose hallmark is the unification of soft SUSY breaking (SSB) parameters renormalized at a scale $Q \simeq M_{\rm GUT}$ to $M_{\rm Planck}$, has served as the paradigm for many phenomenological analyses of SUSY. Assuming that the radiative electroweak symmetry breaking mechanism is operative [79–85], the observed value of M_Z^2 can be used to fix μ^2, and the framework is completely specified by the well-known parameter set

$$m_0,\ m_{1/2},\ \tan\beta, A_0 \text{ and } \mathrm{sign}(\mu). \tag{3}$$

Typically, the weak scale value of $|\mu|$ is similar in magnitude to $m_{\tilde{g}}$, and the bino is the LSP. However, for any chosen value of $m_{1/2}$, the requirement that electroweak symmetry be correctly broken imposes an upper bound on m_0, since the value of μ^2 becomes negative for yet larger values of m_0. There is thus a contour in the m_0–$m_{1/2}$ plane where $\mu^2 = 0$. For values of m_0 just below this bound, $\mu^2 \ll m_{\tilde{g}}^2$ and μ may be comparable to the SSB bino mass parameter, M_1, so that the lightest neutralino is a mixed bino–higgsino state that can annihilate rapidly in the early universe, mainly via its higgsino content. This is the celebrated HB/FP region of the mSUGRA model [51–53], one of the regions of mSUGRA parameter space where the expected neutralino relic density is consistent with (1) [86, 87]. For parameters in this region, squark masses are in the multi-TeV range, and the reach of

[1] More precisely, when we refer to models satisfying (1) below, we require the neutralino relic density to be close to its measured central value so that the neutralino is the dominant DM component, but strictly satisfying (2). The impact on the LHC reach from b jet tagging is insensitive to the precise value of $\Omega_{\tilde{Z}_1} h^2$.

the LHC is determined by final states from gluino pair production: although the higgsino-like chargino may be light, the mass difference $m_{\widetilde{W}_1} - m_{\widetilde{Z}_1}$ is small, so that leptons from its decays are too soft to increase the reach beyond that obtained via the $E_T^{\rm miss}$ signal from gluino pair production [52, 53, 88]. Since the LSP couples preferentially to the third family via its higgsino component, cascade decays of the gluino to third generation fermions tend to be enhanced. As a result, the requirement of a b-tagged jet in SUSY events reduces SM backgrounds and enhances the LHC reach by 15–20% beyond the reach via the inclusive $E_T^{\rm miss}$ channel in the HB/FP region of the mSUGRA model [65].

We should also mention that the b jet multiplicity may also be enhanced in the mSUGRA model if third generation squarks happen to be light, either because of large bottom quark Yukawa couplings when $\tan\beta$ is large, or because the A_t parameter happens to be "just right" so that $m_{\tilde{t}_1} \ll m_{\tilde{q}}$, and $\tilde{t}_1$ mainly decays via $\tilde{t}_1 \to b\widetilde{W}_1$ and $t\widetilde{Z}_1$, or $\tilde{t}_1 \to bW\widetilde{Z}_1$.

2.2 Inverted mass hierarchy models

The evidence for neutrino oscillations [89–94] and its interpretation in terms of neutrino masses provides strong motivation for considering $SO(10)$ SUSY grand unified theories (GUTS) [95–98]. Each generation of matter (including the sterile neutrino) can be unified into a single **16** dimensional representation of $SO(10)$, while the Higgs superfields $\hat{H}_u$ and $\hat{H}_d$ are both contained in a single **10** dimensional representation, allowing for the unification of both gauge (and separately) Yukawa couplings. $SO(10)$ may either be directly broken to the SM gauge group or by a two step process via an intermediate stage of $SU(5)$ unification. The spontaneous breakdown of $SO(10)$ with the concomitant reduction of rank leaves an imprint on the SSB masses which is captured by one additional parameter M_D^2 with a weak scale magnitude but which can take either sign [99–107]. The model is then completely specified by the parameter set

$$m_{16},\ m_{10},\ m_{1/2},\ M_D^2,\ \tan\beta,\ A_0 \text{ and } \mathrm{sign}(\mu), \tag{4}$$

where we have assumed a common SSB mass parameter m_{16} and a different parameter m_{10} for matter and Higgs fields in the **16** and **10** dimensional representations, respectively. The GUT scale SSB masses for MSSM fields then take the form [99–107]

$$\begin{aligned} m_Q^2 &= m_E^2 = m_U^2 = m_{16}^2 + M_D^2, \\ m_D^2 &= m_L^2 = m_{16}^2 - 3M_D^2, \\ m_N^2 &= m_{16}^2 + 5M_D^2, \\ m_{H_{u,d}}^2 &= m_{10}^2 \mp 2M_D^2. \end{aligned} \tag{5}$$

Unification of the Yukawa couplings is possible for very large values of $\tan\beta$ [108–114].[2]

The $SO(10)$ framework that we have just introduced naturally allows for a phenomenologically interesting class of models in which the ordering of matter sfermion masses is inverted with respect to the order for the corresponding fermions [66–68]. Specifically, in models with Yukawa coupling unification, the choice

$$A_0^2 = 2m_{10}^2 = 4m_{16}^2 \tag{6}$$

for the SSB parameters serves to drive third generation sfermion mass parameters to sub-TeV values, leaving us with first and second generation scalars as heavy as 2–3 TeV. A positive value of $M_D^2 \lesssim (m_{16}/3)^2$ is necessary to obtain radiative electroweak symmetry breaking [69, 70]. The multi-TeV values of first and second generation scalar masses ameliorate the SUSY CP and flavor problems without destroying the SUSY resolution of the gauge hierarchy problem, since the fields with substantial direct couplings to the Higgs sector (gauginos and third generation scalars) have masses below the TeV scale. Because third generation sfermions are significantly lighter than their first/second generation cousins, we may expect that SUSY events are enriched in b- (and possibly t-) quark jets in this scenario.

2.3 Non-universal Higgs mass models

Within the mSUGRA model, if $m_0^2 = m_{H_u}^2$(GUT) is smaller than or comparable to $m_{1/2}^2$, $m_{H_u}^2$ runs to a large negative value at the weak scale. The minimization condition for the (tree level) Higgs scalar potential, which reads

$$\mu^2 = \frac{m_{H_d}^2 - m_{H_u}^2 \tan^2\beta}{\tan^2\beta - 1} - \frac{M_Z^2}{2} \simeq -m_{H_u}^2 - \frac{M_Z^2}{2} \tag{7}$$

(where the last approximation is valid for moderate to large values of $\tan\beta$), then implies that $|\mu| \gg |M_{1,2}|$, so that the LSP is essentially a bino, while the heavier -inos are mainly higgsino-like. A way of avoiding this conclusion is to choose $m_{H_u}^2$(GUT) such that $m_{H_u}^2$ runs to small negative values at the weak scale. Within the mSUGRA model, this can only be realized by choosing $m_0 \gg m_{1/2}$, which gives us the well-studied HB/FP region with MHDM discussed above.

A different way would be to relax the assumed universality [36–43] between the matter scalar and Higgs boson

[2] These studies require only approximate unification of third generation quark Yukawa couplings to allow for threshold effects. It has been argued that *exact* unification of these Yukawa couplings leads to a tension with flavor violation in the B and B_s meson systems, unless sparticles are significantly heavier than ∼1 TeV, or a more complicated flavor structure is introduced into the SUSY-breaking sector [115]. This tension is alleviated if small deviations from exact Yukawa coupling unification are admitted [116].

SSB mass parameters in what has been dubbed the "non-universal Higgs mass" (NUHM) models and adopt a large value for $m_{H_u}^2$(GUT). In order to avoid unwanted flavor changing neutral currents, we maintain a universal value m_0 for matter scalars. The GUT scale value of the SSB down Higgs mass parameter may (may not) be equal to $m_{H_u}^2$ leading to a one (two) parameter extension of the mSUGRA framework that we will refer to as the NUHM1 (NUHM2) model [44, 45]. The NUHM1 model is thus completely specified by the mSUGRA parameter set together with $m_\phi = \text{sign}(m_{H_{u,d}}^2)\sqrt{|m_{H_{u,d}}^2|}$, i.e. by,

$$m_0,\ m_\phi,\ m_{1/2},\ A_0,\ \tan\beta \text{ and } \text{sign}(\mu) \quad \text{(NUHM1)}. \tag{8}$$

If m_ϕ is chosen to be sufficiently larger than m_0, the parameter $m_{H_u}^2$ runs down to negative values but remains small in magnitude so that we obtain MHDM *for any value of* m_0 *and* $m_{1/2}$.[3]

Curiously, the NUHM1 model accommodates another possibility of getting agreement with (1). If $m_\phi < 0$, $m_{H_u}^2$ and $m_{H_d}^2$ both run to large, negative values at the weak scale so that

$$m_A^2 = m_{H_u}^2 + m_{H_d}^2 + 2\mu^2 \simeq m_{H_d}^2 - m_{H_u}^2 - M_Z^2 \tag{9}$$

may be small enough for neutralinos to annihilate via the A and H resonances. Within the NUHM1 framework, the Higgs funnel thus occurs for *all values of* $\tan\beta$. Since the Higgs bosons A and H with relatively small masses are expected to be produced via cascade decays of gluinos and squarks, and since these decay preferentially to third generation fermions, we may once again expect an enhancement of the b and, perhaps also, t jet multiplicity.

The NUHM2 model requires two more parameters than the mSUGRA framework for its complete specification. While these may be taken to be the GUT scale values of $m_{H_u}^2$ and $m_{H_d}^2$, it is customary and more convenient to eliminate these in favor of m_A and μ, and work with the hybrid parameter set

$$m_0,\ m_{1/2},\ m_A,\ \mu,\ A_0,\ \tan\beta \quad \text{(NUHM2)}. \tag{10}$$

This then allows us to adjust the higgsino content of the charginos and neutralinos at will, and furthermore allows for as much freedom in the (tree-level) Higgs sector as in the unconstrained MSSM.

2.4 Low $|M_3|$ dark matter model

Instead of relaxing the universality between scalar masses as in the NUHM model, we may also relax the universality between the gaugino mass parameters. If we adjust the GUT scale value of M_1/M_2, so that $M_1 \simeq M_2$ at the weak scale, we obtain mixed wino DM [59–61]. Since there is no principle that forces M_1/M_2 to be positive, we can instead adjust this ratio so that $M_1 \simeq -M_2$ at the weak scale. In this case the LSP remains a bino with charged and neutral winos close in mass to it and agreement with (1) is obtained via bino–wino co-annihilation [62]. Although collider signatures are indeed altered from mSUGRA expectations, we do not expect any enrichment of the b jet multiplicity in this case.

Although it is not immediately obvious, agreement with (1) is also obtained if we maintain $M_1 = M_2$ at $Q = M_{\text{GUT}}$, but instead *reduce* the value of $|M_3|$. Specifically, for smaller values of $|M_3|$, the (top)-squark mass parameters and also A_t^2 are driven to smaller values at the weak scale. These smaller values of top-squark masses and of A_t^2, in turn, slow down the evolution of $m_{H_u}^2$, so that it runs to negative values more slowly than in the mSUGRA model. As a result, the weak scale value of $m_{H_u}^2$, though negative, has a smaller magnitude than in the mSUGRA case, so that the value of μ^2 is correspondingly reduced [see (7)] and the LSP becomes MHDM [54–57]. This is referred to as the "low $|M_3|$ DM" (LM3DM) model, and the corresponding parameter space is given by

$$m_0,\ m_{1/2},\ M_3,\ A_0,\ \tan\beta,\ \text{sign}(\mu) \quad \text{(LM3DM)}. \tag{11}$$

Here $m_{1/2} > 0$ denotes the GUT scale value of $M_1 = M_2$, while M_3 (which is either positive or negative) denotes the corresponding value of M_3 at the GUT scale. For $m_0 \sim m_{1/2} \lesssim 1$ TeV, the GUT scale value of $|M_3|$ must be *reduced* from its mSUGRA value in order to obtain MHDM, as discussed above. In contrast, if we fix $m_{1/2} \simeq 1$ TeV and take m_0 to be multi-TeV, MHDM is obtained for values $|M_3|/m_{1/2} > 1$. To simplify fine tuning issues, we will confine ourselves to $m_0 \lesssim 1$ TeV, where we can obtain agreement with (1) by reducing the value of $|M_3|$. We may expect an increase in the b-multiplicity from SUSY events at the LHC, because of the enhanced higgsino content of the LSP.

2.5 High M_2 dark matter model

Very recently, it has been pointed out [58] that raising the GUT scale value of M_2 from its unified value of $m_{1/2}$ to about (2.5–3)$m_{1/2}$ for $M_2 > 0$, or to between -2 and -2.5 times $m_{1/2}$ for $M_2 < 0$, also leads to a small value of $|\mu|$, giving rise to a relic density in agreement with (1). The parameter space of this high $|M_2|$ dark matter (HM2DM) model is given by

$$m_0,\ m_{1/2},\ M_2,\ A_0,\ \tan\beta,\ \text{sign}(\mu) \quad \text{(HM2DM)}, \tag{12}$$

where $|M_2|$, the GUT scale value of the wino mass parameter, is dialed to large magnitudes to obtain MHDM. The

[3] Of course, if m_ϕ is chosen to be too large, then $m_{H_u}^2$ does not run to negative values and electroweak symmetry breaking is no longer obtained.

large value of $|M_2|$ causes the Higgs SSB $m_{H_u}^2$ to initially increase from its GUT scale value of m_0^2 as Q is reduced from $M_{\rm GUT}$. Ultimately, however, the usual top quark Yukawa coupling effects take over, causing $m_{H_u}^2$ to evolve to negative values, resulting in the well-known radiative breaking of electroweak symmetry. However, because of its initial upward evolution, the weak scale value of $m_{H_u}^2$ is not as negative as in models with unified gaugino masses, and the value of μ^2 is correspondingly smaller. The neutralino LSP then has a significant higgsino component, and we may expect an enhancement of b jets in SUSY events at the LHC.

3 Event simulation and calculational details

We use ISAJET 7.74 [72] with the toy calorimeter described in Refs. [5–7] for the calculation of the SUSY signal as well as of SM backgrounds in the experimental environment of the LHC. We define jets using a cone algorithm with a cone size $\Delta R = \sqrt{\Delta\eta^2 + \Delta\phi^2} = 0.7$. Hadronic clusters with $E_T > 40$ GeV and $|\eta(\text{jet})| < 3$ are classified as jets. Muons (electrons) are classified as isolated if they have $E_T > 10$ GeV (20 GeV) and visible activity in a cone with $\Delta R = 0.3$ about the lepton direction smaller than $E_T < 5$ GeV. We identify a hadronic cluster with $E_T \geq 40$ GeV and $|\eta(j)| < 1.5$ as a b jet if it also has a B hadron, with $p_T(B) > 15$ GeV and $|\eta(B)| < 3$, within a cone with $\Delta R = 0.5$ of the jet axis. We conservatively take the tagging efficiency[4] $\epsilon_b = 0.5$ at the LHC design luminosity of 100 fb^{-1}/y, and we assume that gluon and light quark jets can be rejected as b jets by a factor $R_b = 150$ (50) if $E_T < 100$ GeV ($E_T > 250$ GeV) and a linear interpolation in between.[5] For jets not tagged as a b jet, we require $E_T(j) \geq 50$ GeV.

Gluino and squark production is the dominant sparticle production mechanism at the LHC for gluino and squark masses up to about 1.8 TeV, if $m_{\tilde{q}} \simeq m_{\tilde{g}}$. If instead squarks are very heavy, gluino pair production will dominate the sparticle production rate up to about $m_{\tilde{g}} \sim 0.8$ TeV. Cascade decays of the parent gluinos and squarks then lead to signals in various multi-jet plus multi-lepton plus $E_T^{\rm miss}$ topologies [120–123]. In some scenarios isolated photons from radiative decays of neutralinos to lighter neutralinos or to an ultra-light gravitino may also be present. Our focus, however, is not on these scenarios, but instead on models of the type discussed in Sect. 2 where b- and/or t-quarks are produced in these cascades at a large rate.

Since SUSY particles are expected to be heavy (relative to SM particles) sparticle production is expected to be signaled by events with hard jets, possibly with hard, isolated leptons and large $E_T^{\rm miss}$. The dominant physics backgrounds to these events with hard jets come from $t\bar{t}$ production, $V + j$ production ($V = W, Z$), VV production and QCD production of light jets, where the $E_T^{\rm miss}$ comes from neutrinos produced by the decays of W or Z bosons or of heavy flavors. Missing E_T may also arise from mismeasurement of jet or lepton transverse momenta and from uninstrumented regions of the detector. These non-physics sources of $E_T^{\rm miss}$ are detector-dependent, and only qualitatively accounted for in our simulation with the toy calorimeter. With the hard cuts that we use to obtain the reach, we expect that the physics backgrounds will dominate the difficult-to-simulate detector-dependent backgrounds, and the results of our analyses of the SUSY reach will be reliable. This expectation is indeed borne out, since results of previous theoretical analyses of the SUSY reach [5–7, 13] compare well with the projected reaches obtained by the CMS [9–11] and ATLAS [8] collaborations. The *gain in reach*, if any, that we obtain from b jet tagging should, if anything, be more reliable than the absolute value of the reach.[6]

In the analysis detailed in the next section, we have examined the reach of the LHC for a wide range of sparticle masses, for the different models introduced in Sect. 2. To facilitate this, we generate signals and backgrounds (calculational details are described below) and only write out events that include at least two jets with $E_T(j) \geq 100$ GeV and $E_T^{\rm miss} \geq 100$ GeV, which we refer to as our basic cuts. The corresponding cross sections for SM events are shown in the second column of Table 1. For low to medium values of the sparticle masses, the sparticle production cross sections are large enough for us to extract the signal above SM backgrounds with relatively soft analysis cuts. For very heavy

[4] Notice that we assume that 50% of b jets with $E_T > 40$ GeV and in the central region will be tagged. This is in contrast to a recent study [117] where the 50% efficiency refers to *all* b jets. Effectively, the efficiency in their study is significantly higher than in this paper. Assuming that this larger tagging efficiency will be attained at the LHC, these authors conclude that requiring three tagged b jets provides the best discrimination between the SM background and the SUSY signal in the HB/FP region of the mSUGRA model.

[5] We have been guided by ATLAS studies of b-tagging efficiencies and corresponding rejection factors in $t\bar{t}H$ and WH production processes. See e.g. [118, 119]. It appears that in the low luminosity environment ($L = 2 \times 10^{33}$ cm^2 s^{-1}), a tagging efficiency of 60% with rejection factors comparable to or better than those we have used appear possible for gluon and light quark jets. While we are not aware of correspondingly detailed studies in the high luminosity environment, there appear to be indications in these same studies that comparable tagging efficiency with a rejection rate that is reduced by a factor ≤ 2 may be possible. In our analysis, we have also ignored the fact that c jets (which should occur in backgrounds at considerably lower rates than gluon or light quark jets) will be much more difficult to discriminate from b jets than light quark and gluon jets.

[6] The absolute reach may also suffer from the fact that SM backgrounds may be somewhat larger than those obtained using shower Monte Carlo programs when proper matrix elements for multi-jet production are included. We expect though that the gain in the reach from b-tagging may again be less sensitive to the inclusion of the proper matrix elements.

Table 1 Cross sections in fb for the SM production of $t\bar{t}$, $W+j$, $Z+j$, VV, and QCD jet events that form the dominant backgrounds to the multi-jet plus $E_T^{\rm miss}$ signal from sparticle production at the LHC. The second column gives the cross section for events with the basic requirements of two jets with $E_T(j) \geq 100$ GeV and $E_T^{\rm miss} \geq 100$ GeV. The last three columns give the corresponding cross sections for the softest of the final set of cuts (listed in the bottom part of Table 2) that we actually use in our analysis, with no requirement of b jet tagging (column 3), requiring at least one tagged b jet (column 4) and at least two tagged b jets (column 5). For illustration, we also list the corresponding signal cross sections for two points in the HB/FP region of the mSUGRA model, with $A_0 = 0$, $\tan\beta = 10$ and $m_{\tilde{g}} \simeq 1$ TeV, $m_{\tilde{q}} \sim 3$ TeV (mSUGRA1) and $m_{\tilde{g}} \simeq 1.5$ TeV and $m_{\tilde{q}} \sim 3.9$ TeV (mSUGRA2)

Source	$\sigma_{\rm basic}$	$\sigma_{\rm cut}(0b)$	$\sigma_{\rm cut}(1b)$	$\sigma_{\rm cut}(2b)$
$t\bar{t}$	19900	2.16	1.41	0.365
$W+j$	21400	12.0	1.36	0.133
$Z+j$	8850	5.11	0.059	0.0052
VV	89.8	0.0248	0.0020	0.0001
QCD	93700	11.6	3.11	0.467
Total	1.44×10^5	30.9	5.94	0.97
mSUGRA1	261	12.0	9.26	3.86
mSUGRA2	48.4	2.44	1.95	0.87

sparticles, however, the production rate is small, but essentially all events contain very energetic jets and large $E_T^{\rm miss}$. The detection of the signal is then optimized by using very hard cuts that strongly suppress SM backgrounds, while retaining the bulk of the SUSY signal. Since our aim is to develop a strategy that can be applied to essentially the entire interesting mass range of a wide variety of models, we are led to evaluate the signal together with the SM background for a wide range of cuts, listed in detail in the next section. To understand the relative importance of the different background sources, in the last three columns of Table 1 we list the corresponding cross sections for the *softest* set of cuts that we use in our analysis, as described in detail in Sect. 4.

In the last two rows we also list the corresponding signal cross sections for two WMAP-consistent cases in the HB/FP region of the mSUGRA model. Several comments are worth noting.

- We see that with the basic requirements of two jets with $E_T \geq 100$ GeV and $E_T^{\rm miss} \geq 100$ GeV, the background is two (three) orders of magnitude larger than the signal for $m_{\tilde{g}} \simeq 1$ (1.5) TeV; however, the analysis cuts very efficiently reduce the background, while reducing the signal by a much smaller factor.
- After these analysis cuts we see that QCD, followed by $V+j$ production, are the leading backgrounds to the inclusive $E_T^{\rm miss}$ signal. Top pair production, while significant, is considerably smaller. Since we do not require the presence of leptons, the background from VV production is negligible.
- The backgrounds from QCD and $V+j$ production may be sharply reduced by the use of b jet tagging with a relatively small loss of the signal. In contrast, since top events necessarily contain b jets, b-tagging reduces the $t\bar{t}$ background only by a modest amount.

Table 1 highlights the importance of a careful evaluation of the QCD and the $V+j$ backgrounds. This is technically complicated, because the large size of the cross sections necessitates simulations of a very large number of events to obtain a reliable estimate for the backgrounds after the very hard cuts that are needed for optimizing the reach of the LHC.[7] Moreover, since the cross section is a rapidly falling function of the center of mass energy, or equivalently, the hard-scattering p_T of the initial partons, we must ensure that our procedure generates events even for very large values of $P_T^{\rm HS}$ where the matrix element is very small, so that these events, which have much smaller weights, are included in the analysis. To facilitate this, we have generated the various backgrounds using different numbers, $N_i^{\rm HS}$, of hard-scattering bins: the bin intervals are finely spaced for low values of $P_T^{\rm HS}$, where event weights are very large. We choose $N_i^{\rm HS} = 53, 13, 8$ and 7 for $i =$ QCD, $V+j$, $t\bar{t}$ and VV, respectively, where the choice $N_{\rm HS}^{\rm QCD} = 53$ reflects the largeness of the QCD cross section. We have generated a total of about 10M QCD events, about 1M $W+j$ events and about 500–700K events for each of the other backgrounds. If, for any set of cuts, we find zero events in our simulation of a particular background, we set this background cross section to a value corresponding to the one event level in the bin with the smallest weight in our simulation.

4 Bottom jet tagging and the reach of the LHC

4.1 Simulation of the signal and the LHC reach

Simulation of the signal events is technically much easier than that of the background. This is largely because the signal typically originates in heavy sparticles and so passes the hard analysis cuts with relative ease, compared to the background. To assess how much b jet tagging extends the SUSY reach of any particular model, rather than perform extensive and time-consuming scans of the parameter space, we have defined "model lines" along which the sparticle mass scale increases. We then choose parameters along these lines, and for every such parameter set use ISAJET 7.74 to generate a SUSY event sample. Next, we pass this event sample through the set of analysis cuts defined below, and we define

[7] Of course, the fact that we are far into the tails of these backgrounds where the simulations (which will be tuned to the data when these become available) require possibly unjustified extrapolations is a different matter.

the signal to be observable at the LHC if for *any* choice of cuts

- the signal exceeds 10 events, assuming an integrated luminosity of 100 fb^{-1},
- the statistical significance of the signal $N_{\rm signal}/\sqrt{N_{\rm back}} \geq 5$, and
- the signal to background ratio, $N_{\rm signal}/N_{\rm back} \geq 0.25$.

We also require a minimum of 15 events after cuts in our simulation of the signal. We obtain the reach for each model line by comparing the corresponding signal with the background, and ascertaining where the signal just fails our observability criteria for *the entire set of cuts in Table 2* below.

4.2 Analysis cuts

The inverted mass hierarchy model based on $SO(10)$ SUSY GUTs, whose hallmark is the light third generation, serves as the prototypical case where we expect enhanced b jet multiplicity in SUSY events. We have used this framework to guide us to the set of analysis cuts that can be used for the optimization of the SUSY signal for a wide range of sparticle masses in a wide class of models. Toward this end, we fix $\mu < 0$, $A_0 < 0$, and $\tan\beta = 47$ (a large value is needed for the unification of Yukawa couplings) and choose $m_{10} = \sqrt{2}m_{16}$, $A_0 = -2m_{16}$ to obtain the hierarchy between the first/second and third generation scalars as discussed above. The choice $M_D = 0.25m_{16}$ facilitates electroweak symmetry breaking. We vary the gluino mass along the "model line" with $m_{1/2} = 0.36m_0 + 48$ GeV, which maintains a hierarchy between the generations. The value of

$$S \equiv \frac{3(m^2_{\tilde{u}_L} + m^2_{\tilde{d}_L} + m^2_{\tilde{u}_R} + m^2_{\tilde{d}_R}) + m^2_{\tilde{e}_L} + m^2_{\tilde{e}_R} + m^2_{\tilde{\nu}_e}}{3(m^2_{\tilde{t}_1} + m^2_{\tilde{b}_1} + m^2_{\tilde{t}_2} + m^2_{\tilde{b}_2}) + m^2_{\tilde{\tau}_1} + m^2_{\tilde{\tau}_2} + m^2_{\tilde{\nu}_\tau}}$$

is typically around 3.5–4.1 along this model line.

The optimal choice of cuts depends on the (a priori unknown) sparticle spectrum, and to a smaller extent on their decay patterns. While hard cuts optimize the signal if sparticles are heavy, these would drastically reduce (or even eliminate) the signal if sparticles happen to be light. In order to obtain a general strategy that can be used for a wide variety of models, we have used the $SO(10)$ model with $\mu < 0$ to devise a universal set of cuts that can be used for SUSY discovery in any of the various models that we have introduced, and likely, also for a wider class of models.

Toward this end, we generate a sample of signal events for this "test model line" and run this, as well as the SM backgrounds that we discussed above, through each one of the large set of analysis cuts detailed in the upper part of Table 2. Here, $m_{\rm eff}$ is the scalar sum of the transverse ener-

Table 2 The complete set of cuts that we examined for extraction of the SUSY signal over the SM backgrounds is shown in the upper part of the Table. The $0b$, $1b$ and $2b$ entries respectively denote requirements for events without any restriction on b jet tagging, with at least one tagged b jet, and with at least two tagged b jets. The lower part of the table shows the final set of cuts that we recommend for the extraction of the SUSY signal over the entire range of masses and models that we have explored in the paper

Variable	$0b$, $1b$	$2b$
$E_T^{\rm miss}$ (GeV) $>$	300, 450, 600, 750, 900, 1050	300, 450, 600, 750, 900, 1050
$E_T(b_1)$ (GeV) $>$	40, 100, 200, 300, 400	40, 100, 200, 300, 400
$m_{\rm eff}$ (GeV) $>$	1500, 2000, 2500, ..., 4000	1500, 1750, 2000, 2250, 2500, 2750
$\Delta\phi <$	180°, 160°, 140°	180°, 160°, 140°
$\Delta\phi_b <$	n/a	180°, 150°, 120°
$n_j \geq$	4, 5, 6, 7, 8	4, 5, 6, 7, 8
$S_T \geq$	0.1, 0.2	0.1, 0.2
$[E_T(j_1), E_T(j_2)]$ (GeV) $>$	(300, 100), (300, 200), (400, 200), (400, 300), (500, 200), (500, 300), (500, 400), (600, 200), (600, 300), (600, 400), (600, 500), (700, 200), (700, 300), (700, 400), (700, 500), (700, 600), (800, 200), (800, 300), (800, 400), (800, 500), (800, 600)	
	Final cuts	
$E_T^{\rm miss}$ (GeV) $>$	450, 600, 750, 900,	450, 600, 750
$E_T(b_1)$ (GeV) $>$	40, 100, 200	40, 100, 200, 300
$m_{\rm eff}$ (GeV) $>$	1500, 2000, 2500, ..., 4000	1500, 1750, 2000, 2250
$\Delta\phi <$	180°, 160°, 140°	180°
$\Delta\phi_b <$	n/a	180°, 150°, 120°
$n_j \geq$	4, 5, 6, 7, 8	4, 5, 6, 7
$S_T \geq$	0.1	0.1
$[E_T(j_1), E_T(j_2)]$ (GeV) $>$	(300, 200), (400, 200), (500, 200), (500, 300), (500, 400), (600, 200), (600, 500), (700, 300), (700, 600), (800, 300), (800, 600)	

gies of the four hardest jets in the event combined with the missing transverse energy, $\Delta\phi$ is the transverse plane opening angle between the two hardest jets, and $\Delta\phi_b$ the corresponding angle between the two tagged b jets in events with $n_b \geq 2$. To clarify, the softest set of cuts that we use for the $0b$ signal has $[E_T^{\rm miss}, E_T(j_1), E_T(j_2), E_T(b_1), m_{\rm eff}] \geq [300, 300, 100, 40, 1500]$ GeV, $n_j \geq 4$ and transverse sphericity $S_T > 0.1$, with no restriction on jet opening angles. Next, we harden the cut on one of these observables to the next level, keeping the others at the same value, etc., until the complete set of $6 \times 5 \times 6 \times 3 \times 3 \times 5 \times 2 \times 21$ combinations has been examined for $n_b \geq 2$. Since there are no tagged b jets (or there is just one) in the $n_b = 0$ ($n_b = 1$) case, there are correspondingly fewer combinations for these analyses.

For each of these cut choices, we analyzed the observability and statistical significance of the LHC signal for our test $SO(10)$ model line for an integrated luminosity of 100 fb^{-1}. We found that the subset of cuts shown in the lower part of Table 2 (and labeled "Final Cuts") is sufficient to ensure the observability of the SUSY signal over the entire mass range. Restricting the analysis to this subset has no impact on either the observability or the statistical significance of the signal over the entire sparticle mass range. In the remainder of this paper we, therefore, confine ourselves to this limited subset of cuts, as this speeds up the analysis considerably.

4.3 Results

In this section, we evaluate prospects for increasing the reach of the LHC by the use of b-tagging to reduce SM backgrounds, thereby increasing the statistical significance of the SUSY signal, for each of the models introduced in Sect. 2. We confine ourselves to various one-parameter model lines (introduced below) along which sparticle masses increase and run the signal and backgrounds through each of the final set of cuts in Table 2, and we optimize the signal by selecting the cut choice that yields an observable signal with the highest statistical significance. To assess the gain from b-tagging, for each model line we first do so without any requirement on b-tagging, and then repeat it requiring, in addition, at least one and at least two tagged b jets.

4.3.1 The HB/FP region of the mSUGRA model

The possibility of increasing the LHC reach was first studied in the HB/FP region of the framework of mSUGRA [65], where it was found that the reach could be increased by up to 15–20%. We have repeated this study, albeit with a somewhat different model line with

$$m_{1/2} = 0.295 m_0 - 507.5 \text{ GeV},$$
$$\tan\beta = 30, \qquad A_0 = 0,$$

in the HB/FP region that saturates the relic density in (1) and, of course, with the different set of cuts that we use here. We find an increased reach from b-tagging in qualitative agreement with Ref. [65].

4.3.2 Inverted mass hierarchy model

As discussed in Sect. 4.2, we have already used the $SO(10)$ model with $\mu < 0$ and parameters related by (6), where we obtain an inverted mass hierarchy to choose the final set of cuts for our analysis. Here, we show results for the reach of the LHC with and without requirements of b jet tagging for two model lines with a significant inversion of the sfermion mass hierarchy; one for each sign of μ. For both of these, we choose

$$-A_0 = 2m_{16} = \sqrt{2} m_{10}, \qquad \tan\beta = 47, \tag{13}$$

with

$$M_D = 0.25 m_{16} \quad \text{and}$$
$$m_{1/2} = 0.36 m_{16} + 48 \text{ GeV} \quad \text{for } \mu < 0, \tag{14}$$

$$M_D = 0.20 m_{16} \quad \text{and}$$
$$m_{1/2} = 0.30 m_{16} + 39 \text{ GeV} \quad \text{for } \mu > 0. \tag{15}$$

Of course, to determine the reach for the $\mu < 0$ model line we generate sets of signal events different from those used in Sect. 4.2.

Our results are shown in Fig. 1, where we plot the largest statistical significance of the signal, $N_{\rm signal}/\sqrt{N_{\rm back}}$, versus the corresponding gluino mass for (a) $\mu < 0$, and (b) $\mu > 0$, assuming an integrated luminosity of 100 fb^{-1}. The maximal $N_{\rm signal}/\sqrt{N_{\rm back}}$ was obtained running over all the cuts in Table 2, subject to the requirement that the $N_{\rm signal}/N_{\rm back} > 0.25$ and $N_{\rm signal} > 10$ event criteria are satisfied. The solid (red) curves show this significance for the inclusive $E_T^{\rm miss}$ signal with no requirement of b jet tagging, while the dashed (black) curve and the dotted (blue) curves correspond to cases in which we require at least one and two tagged b jets, respectively. The wiggles in these curves reflect the statistical errors in our simulation. We attribute the somewhat larger reach in the left frame to the fact that the mass hierarchy (as measured by the value of S) is somewhat smaller for $\mu < 0$, so that $\tilde{q}\tilde{g}$ makes a larger contribution in this case. We also see that for $\mu < 0$, b-tagging leads to an increase of the LHC reach by ∼200 GeV, or about 10%, while the corresponding increase is somewhat smaller for the model line with positive μ.

This difference (which may well be not very significant in view of the wiggles) is evidently due to the increased reach in the $2b$ channel and could arise from a complicated interplay between the effect of cuts and the sparticle spectrum:

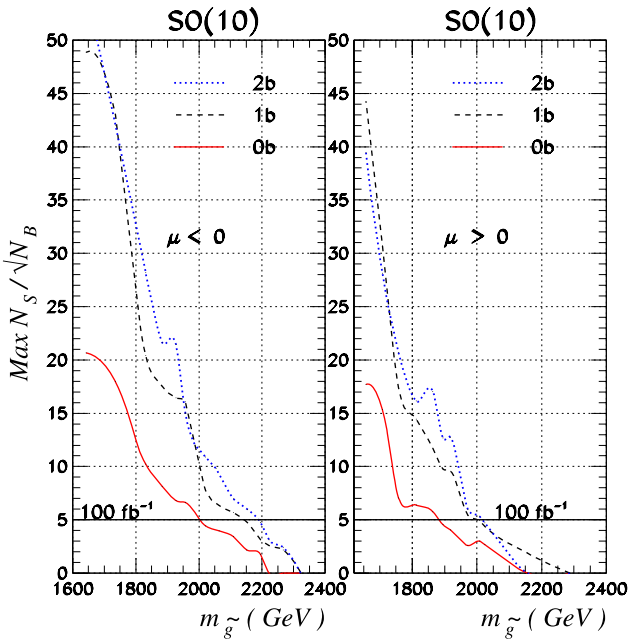

Fig. 1 The statistical significance of the SUSY signal satisfying our observability criteria at the LHC for the inverted hierarchy $SO(10)$ model lines introduced in the text, assuming an integrated luminosity of 100 fb^{-1} for (**a**) $\mu < 0$, and (**b**) $\mu > 0$. The *solid* (*red*) *line* is for the signal with no requirement on b-tagging, the *dashed* (*black*) *line* is with the requirement of at least one tagged b jet, and the *dotted* (*blue*) *line* is with at least two tagged b jets. The signal is observable if the statistical significance is above the *horizontal line* at $N_{\text{signal}}/\sqrt{N_{\text{back}}} = 5$

for instance, for $m_{\tilde{g}} \sim 1960$ GeV, $m_{\tilde{b}_1}$ is significantly lighter in the $\mu < 0$ case, while $m_{\tilde{t}_1}$ is considerably heavier. As a result, the branching fraction for the decays $\tilde{g} \to b\tilde{b}_i$, which likely leads to a harder spectrum for b jets (compared to $\tilde{g} \to t\tilde{t}_1$, which constitutes the bulk of the remaining decays of the gluino), falls from 38% for negative μ to 28% for positive μ.

4.3.3 *Non-universal Higgs mass models*

Next we turn to the impact of b-tagging on the reach in NUHM models with just one additional parameter m_ϕ that is adjusted so that agreement with the observed relic density is obtained. This may be done either by tempering the LSP content so that it is MHDM ($m_\phi > m_0$), or by adjusting the masses so that the LSP annihilation rate is resonantly enhanced by the exchange of neutral A or H bosons in the s-channel ($m_\phi < 0$). We did not study the NUHM model in which both Higgs SSB mass parameters are arbitrary—the so-called NUHM2 models in the nomenclature of Ref. [44, 45]—because this meant that both m_A and μ are arbitrary, resulting in too much freedom for a definitive analysis. Beginning with the MHDM cases of the LSP where sparticle decays to third generation quarks are enhanced by the higgsino content of the LSP, we introduce two model lines with $A_0 = 0$, $\tan\beta = 10$ and $\mu > 0$, with (1) $m_0 = m_{1/2}$, and (2) $m_0 = 3m_{1/2}$, for which we have to choose $m_\phi \simeq 1.7m_0$ and $m_\phi \simeq 1.12m_0$, respectively, in order to obtain the observed relic density. In the former case, the squarks of the first two generations are roughly degenerate with the gluinos, whereas in the latter case $m_{\tilde{q}} \sim 1.6m_{\tilde{g}}$.

Our results for the statistical significance of the LHC SUSY signal, with and without b jet tagging, are shown in Fig. 2 for (a) $m_0 = m_{1/2}$, and (b) $m_0 = 3m_{1/2}$. We see that, while b-tagging clearly improves the reach by ∼10% in the case shown in frame (b), it leads to a *degradation* of the reach in frame (a). We have traced this to the fact that for this case, where squark and gluino masses are comparable, squark production (particularly first generation squark production) makes a significant contribution to the signal after the hard cuts. Since these squarks dominantly decay to charginos and neutralinos (remember that because $m_{\tilde{q}} \sim m_{\tilde{g}}$, the decay $\tilde{q} \to q\tilde{g}$ is suppressed by phase space) plus *quarks of their own generation,* there are essentially no b-quarks produced in squark decays, and a sizable fraction of the inclusive E_T^{miss} signal is actually cut out by any b-tagging requirement. In frame (b), the squarks are much heavier than gluinos and so contribute a smaller fraction of the signal, but more relevantly, $\tilde{q} \to q\tilde{g}$ with a large branching fraction, so that b-tagging helps in this case. These considerations also explain why the increase in reach from b-tagging is not as large as in the case of the HB/FP region of the mSUGRA model where $m_{\tilde{q}} \gg m_{\tilde{g}}$ [65].

We now turn to the $m_\phi < 0$ model line shown in Fig. 2c for which we have chosen $m_0 = 5m_{1/2}$ (to ensure squark contributions to the signal do not dilute the effect of b tagging as in the case that we just discussed), $A_0 = 0$, $\tan\beta = 20$ and $\mu > 0$, and m_ϕ is adjusted to be about $-1.47m_0$ to give agreement with (1) via resonant annihilation of LSPs through A/H exchanges in the s-channel. This means that A and H must be relatively light and accessible in cascade decays of gluinos and squarks. However, we see no enhancement of the LHC reach in this case. We understand this in hindsight. In this case $|\mu|$ is large, so the lighter neutralinos produced in gluino cascade decays are gaugino-like, with $m_{\widetilde{W}_1} \simeq m_{\widetilde{Z}_2} \simeq 2m_{\widetilde{Z}_1}$. Then the very condition $2m_{\widetilde{Z}_1} \sim m_A$ that makes the LSP annihilation cross section resonant suppresses the phase space for the decays of $\widetilde{Z}_2 \to A$ or $H + \widetilde{Z}_1$, so that these are not significantly produced in cascade decays of gluinos. Since squarks are very heavy, they are essentially irrelevant to this discussion.

4.3.4 *Low M_3 dark matter model*

As explained above, we can also obtain MHDM, and hence a potential increase in reach via b-tagging, in models with non-universal gaugino mass parameters, where $|M_3(\text{GUT})|$ is taken to be reduced compared to its value in models with

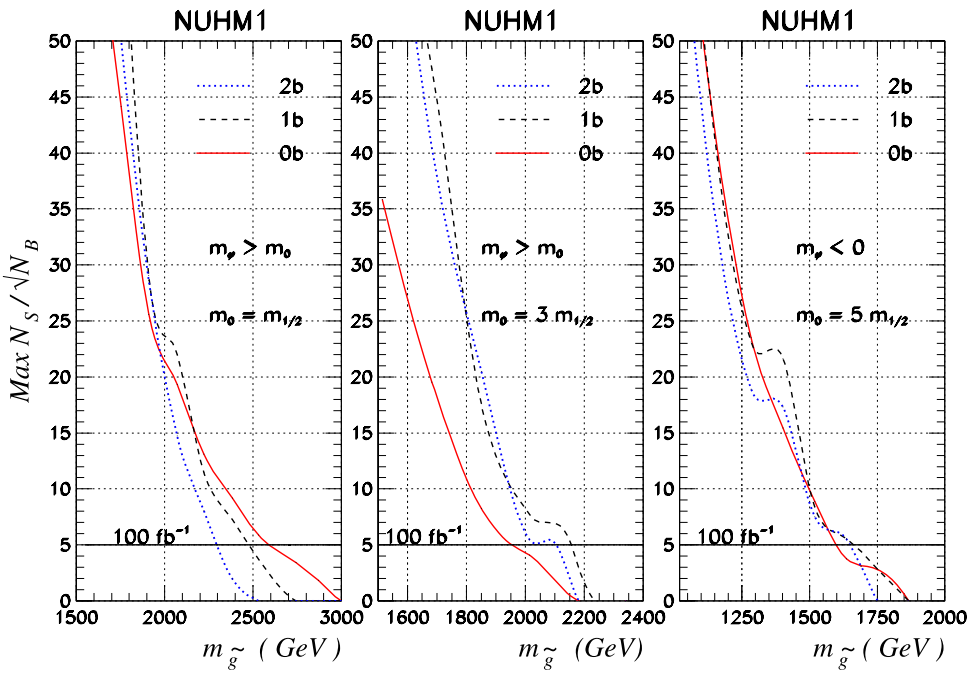

Fig. 2 The statistical significance of the SUSY signal satisfying our observability criteria at the LHC for the three NUHM model lines introduced in the text, assuming an integrated luminosity of 100 fb^{-1}. All the model lines have $A_0 = 0$ and $\mu > 0$, with (**a**) $m_\phi > 0$, $\tan\beta = 10$, $m_0 = m_{1/2}$, (**b**) $m_\phi > 0$, $\tan\beta = 10$, $m_0 = 3m_{1/2}$, and (**c**) $m_\phi < 0$, $\tan\beta = 20$, $m_0 = 5m_{1/2}$. The *solid* (*red*) *line* is for the signal with no requirement on b-tagging, the *dashed* (*black*) *line* is with the requirement of at least one tagged b jet, and the *dotted* (*blue*) *line* is with at least two tagged b jets. The signal is observable if the statistical significance is above the *horizontal line* at $N_{\rm signal}/\sqrt{N_{\rm back}} = 5$

gaugino mass unification. To study the gain in the reach that we may obtain in this case, we have explored an LM3DM model line with

$$m_0 = m_{1/2}, \qquad A_0 = 0, \qquad \tan\beta = 10, \qquad \mu > 0,$$

where the GUT scale value of M_3 (which we take to be positive) is adjusted to saturate the measured CDM relic density.[8]

The corresponding dependence of the statistical significance of the SUSY signal on $m_{\tilde{g}}$ is shown in Fig. 3. We see that in this case b-tagging leads to an increase in reach close to 15%. This is because though gluinos and squarks are both reduced in mass relative to their uncolored cousins, the reduced value of the gluino mass parameter leads to $m_{\tilde{q}} \sim (1.4\text{–}1.5)m_{\tilde{g}}$ even for $m_0 = m_{1/2}$, to be compared to $m_{\tilde{q}} \sim m_{\tilde{g}}$ that we obtained for models with unified gaugino masses as e.g. in the NUHM case just discussed. The large value of $m_{\tilde{q}}$ relative to $m_{\tilde{g}}$ then leads to an enhanced reach via b-tagging just as before.

4.3.5 *High M_2 dark matter model*

As a final example, we consider the LHC reach in the HM2DM model, where agreement with (1) is obtained by raising $|M_2(\text{GUT})|$ from its canonical value of $m_{1/2}$ in models with gaugino mass unification, so that the lightest neutralino is MHDM. Since the LSP contains a substantial higgsino component, it is again reasonable to expect that b jet

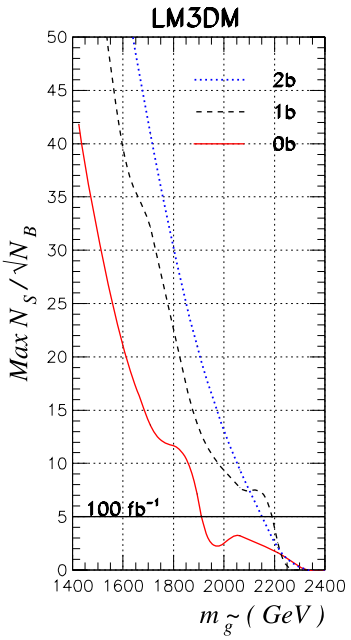

Fig. 3 The statistical significance of the SUSY signal satisfying our observability criteria at the LHC for the LM3DM model line with $m_0 = m_{1/2}$, $A_0 = 0$, $\tan\beta = 10$ and $\mu > 0$, where $M_3(\text{GUT})$ is adjusted to saturate the measured CDM relic density, assuming an integrated luminosity of 100 fb^{-1}. The *solid* (*red*) *line* is for the signal with no requirement on b-tagging, the *dashed* (*black*) *line* is with the requirement of at least one tagged b jet, and the *dotted* (*blue*) *line* is with at least two tagged b jets. The signal is observable if the statistical significance is above the *horizontal line* at $N_{\rm signal}/\sqrt{N_{\rm back}} = 5$

[8] Roughly speaking, for $m_0 = m_{1/2} = 700$ GeV, $M_3(\text{GUT}) = 277$ GeV, and for an increase of δm_0 in $m_0 = m_{1/2}$, the GUT scale value of M_3 has to be raised by about $\delta M_3 \sim \delta m_0/2.25$.

tagging may increase the SUSY reach of the LHC. As we have already seen in other examples, the increased reach from b jet tagging depends on the value of the squark mass relative to $m_{\tilde{g}}$. This led us to consider two model lines with, (a) $m_0 = m_{1/2}$, and (b) $m_0 = M_2$(GUT), for both of which we take $\tan\beta = 10$, $\mu > 0$ and $A_0 = 0$. Since the correct relic density is obtained by *raising* M_2, model line (b), which gives heavier squarks than model line (a), will give a smaller reach as measured in terms of $m_{\tilde{g}}$. The *increase* in the reach from b jet tagging will, however, be larger for model line (b), since squark contributions to sparticle production are kinematically suppressed.

The statistical significance of the SUSY signal in the HM2DM model is shown for the two model lines in the two frames of Fig. 4. Indeed we see that while the reach in the left frame for $m_0 = m_{1/2}$ extends to $m_{\tilde{g}} \leq 2.5$ TeV (as compared to 2.1 TeV in the right frame), there is very little gain in the reach from b jet tagging in this case, where squark and gluino masses are comparable. This is in contrast to the gain in reach of ∼8% for the case of heavier squarks in the right hand frame.

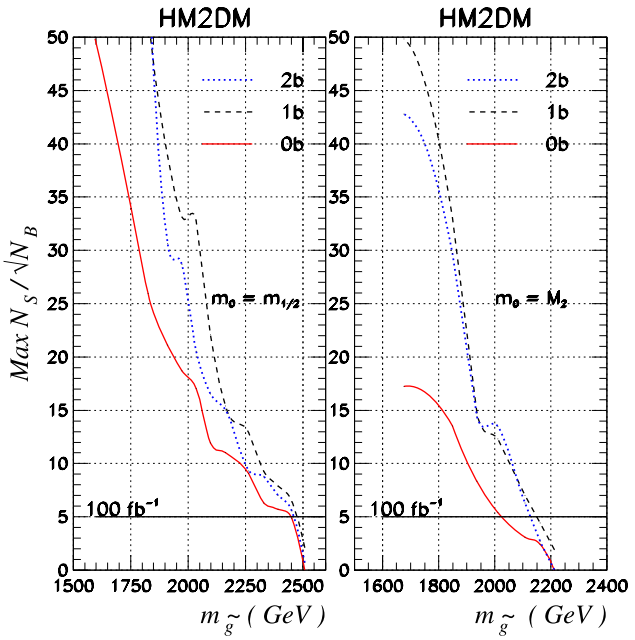

Fig. 4 The statistical significance of the SUSY signal satisfying our observability criteria at the LHC for the HM2DM model line with $A_0 = 0$, $\tan\beta = 10$, $\mu > 0$ and (a) $m_0 = m_{1/2}$, and (b) $m_0 = M_2$(GUT). In both frames, M_2(GUT) is adjusted to a positive value so as to saturate the measured CDM relic density, and an integrated luminosity of 100 fb^{-1} is assumed. The *solid* (*red*) *line* is for the signal with no requirement on b-tagging, the *dashed* (*black*) *line* is with the requirement of at least one tagged b jet, and the *dotted* (*blue*) *line* is with at least two tagged b jets. The signal is observable if the statistical significance is above the *horizontal line* at $N_{\rm signal}/\sqrt{N_{\rm back}} = 5$

5 Top tagging and the reach of the LHC

We have seen that requiring a b-tagged jet reduces the SM background relative to the SUSY signal in a wide variety of models, and so increases the SUSY reach of the LHC. This then raises the question of whether it is possible to further increase this reach by requiring a top-tagged jet, since the mechanisms that serve to enhance the decays of SUSY particles to b-quarks frequently tend to enhance decays to the entire third generation of SM fermions. SM backgrounds to $E_T^{\rm miss}$ events with t-quarks should, of course, be smaller than those for events with b-quarks. In this section, we study the prospects for top tagging, once again using the inverted mass hierarchy model line (14) to guide our thinking.

Top tagging in SUSY events has been suggested previously for the reconstruction of SUSY events, assuming that $\tilde{t}_1$ or $\tilde{b}_1$ are light enough so that $\tilde{g} \to t\tilde{t}_1 \to tb\widetilde{W}_1$ and/or $b\tilde{b}_1 \to bt\widetilde{W}_1$ occur with large branching fractions [124, 125]. Using a top reconstruction procedure described below, together with an estimate of fake tops from an analysis of side-bands, it was shown that for $m_{\tilde{g}} \sim 700$ GeV, for which the SUSY event rate is very large, partial reconstruction of SUSY events with gluinos decaying to third generation squarks was possible at the LHC.

We follow the approach developed in this study to reconstruct the top quark via its hadronic decay mode. In a sample of multi-jet + $E_T^{\rm miss}$ events with at least one tagged b jet, we identified a hadronically decaying top by first identifying all pairs of jets (constructed from those jets that are not tagged as b jets) as a hadronically decaying W if $|m_{jj} - M_W| \leq 15$ GeV. We then pair each such W with the tagged b jet(s) and identify any combination as a top if $|m_{bW} - m_t| \leq 30$ GeV. If we can reconstruct such a "top", we defined the event to be a top-tagged event. The efficiency for tagging tops in this way turns out to be small.[9]

For our examination of the impact of top tagging on the SUSY reach of the LHC, we have again chosen the $SO(10)$ model line (14) with $\mu < 0$ as a test case. In this case,

[9] In a simulated sample of about 90K $t\bar{t}$ pairs with a hard-scattering E_T between 50–400 GeV, we found only 6,255 top tags even with $\epsilon_b = 1$. To understand this large loss of efficiency we note that first, leptonically decaying tops (branching fraction of ∼1/3) are clearly not identified. Second, b jets are within their fiducial region ($E_{Tj} > 40$ GeV, $|\eta_j| \leq 1.5$, with a B-hadron with $p_T(B) \geq 15$ GeV within a cone of $\Delta R = 0.5$ of the jet axis) only about 5/8 of the time. Third, it is necessary for the top with the b jet inside the fiducial region to decay hadronically in order to make the top mass window, since the wrong combination mostly falls outside it. Finally, if the jets from the W from the top with the tagged b merge or radiate a separate jet at a large angle, this W is lost, and hence the top is not tagged. We have checked with our synthetic top sample that the choice of mass bins of ±15 GeV about M_W and ±30 GeV about m_t suggested in Refs. [124, 125] does not lead to loss of signal from events where the top decays hadronically into well separated jets: most of the loss in efficiency comes from the other factors given details of above.

Table 3 The complete set of cuts examined for the extraction of the SUSY signal with tagged t jets. In addition to the basic cuts detailed in the text, we require that $S_T \geq 0.1$

Variable	Values
$E_T^{\rm miss}$(GeV) $\geq$	300, 400, ..., 900
$m_{\rm eff}$(GeV) $\geq$	800, 900, ..., 2000
$n_j \geq$	3, 4, ..., 8
$n_b \geq$	1

since other squarks are heavy, the gluino mainly decays with roughly equal likelihood via $\tilde{g} \to \tilde{t}_1 t$ and $\tilde{g} \to \tilde{b}_1 b$, where subsequent decays of the third generation squarks can lead to yet more top quarks in SUSY events. As for the case of b jet tagging, we have run the SUSY sample through a set of cuts shown in Table 3 to optimize our top-tagged signal relative to SM background. Because of the small efficiency for top tagging we cannot, however, afford a large reduction of the signal from multiple cuts. We have, therefore, restricted our optimization to cuts on just the three variables $E_T^{\rm miss}$, $m_{\rm eff}$ and n_j, imposing the basic requirements on the observability of the signal discussed in Sect. 3.

Table 4 A comparison of the statistical significance of the LHC signal using top tagging described in the text, for three different cases along the $SO(10)$ model line (14), with other parameters as fixed by (13). The first few lines show the value of m_{16} along with sample particle masses and branching fractions. The next three lines show the choice of cuts for the variables in Table 3 that maximizes the statistical significance of the top-tagged signal. The signal and SM background cross sections for these cuts are shown on the next two lines for the cut choice that leads to an observable signal with the greatest statistical significance. The last three rows compare the statistical significance of the signal using top tagging with that obtained using b jet tagging discussed in Sect. 4

	Case 1	Case 2	Case 3
m_{16} (GeV)	1650	1770	1820
$m_{\tilde{g}}$ (GeV)	1522	1614	1661
$m_{\tilde{u}_R}$ (GeV)	2108	2255	2319
$m_{\tilde{t}_1}$ (GeV)	714	766	792
$m_{\tilde{b}_1}$ (GeV)	744	842	876
$m_{\widetilde{W}_1}$ (GeV)	533	570	589
$m_{\widetilde{Z}_1}$ (GeV)	279	299	309
$B(\tilde{t}_1 \to t\widetilde{Z}_i)$	0.64	0.69	0.70
$B(\tilde{b}_1 \to t\widetilde{W}_1)$	0.37	0.31	0.30
$E_T^{\rm miss}$ (GeV) $\geq$	300	500	n/a
$m_{\rm eff}$ (GeV $\geq$	1700	800	n/a
$n_j \geq$	8	3	n/a
$\sigma_{\rm SUSY}$ (fb)	0.138	0.108	n/a
$\sigma_{\rm back}$ (fb)	0.0117	0.0306	n/a
$N_{\rm SUSY}/\sqrt{N_{\rm back}}$			
top tag	12.7	6.14	0.00
$1b$	62.8	52.5	44.7
$2b$	93.5	64.0	46.4

The results of our SUSY reach analysis with top tagging are summarized in Table 4. Here, we show the optimized statistical significance of the SUSY signal for three cases in the vicinity of the ultimate reach using this technique. In this table, we show representative sparticle masses along with branching fractions for sparticle decays that lead to top quark production in SUSY cascades. We then give details on the final choice of cuts that optimizes the top-tagged SUSY signal. We also show the top-tagged signal cross section after these cuts along with the corresponding SM background, and the statistical significance of the top-tagged signal achieved in cases 1 and 2; for case 3, the signal is not observable by our criteria. Finally, in the last two rows we show the corresponding statistical significance using b jet tagging discussed in Sect. 4. We see from the table that, while top tagging allows an LHC reach for $m_{\tilde{g}}$ just above 1600 GeV, *the top-tagged rate becomes too low* for heavier gluinos. In contrast, b jet tagging yields a statistical significance in excess of 50 close to the top-tagged reach. We thus conclude that while top tagging can be used as a diagnostic tool, or even for a reconstruction of SUSY events [124, 125] in favorable cases, it will not extend the SUSY reach of the LHC.

6 Can we directly detect third generation squarks?

In models in which the third generation is significantly lighter than the other generations, it is natural to ask whether it is possible to detect signals from the *direct production* of third generation squarks. As already mentioned, their detection as secondaries from production and subsequent decays of gluinos is possible if the gluino itself is not very heavy [124, 125]. Our goal, therefore, is to examine whether the signal from the direct production of third generation squarks can be separated both from SM backgrounds, as well as from production of other SUSY particles. Clearly, this is a model-dependent question, since the SUSY "contamination" to the third generation signal will depend strongly on the masses of the other squarks and the gluino. In this section, we will study this issue within the context of the inverted mass hierarchy model with $\mu < 0$, which we have used as our canonical test case.

Since there are essentially no third generation quarks in the proton, the cross section for third generation squarks falls rapidly with the squark mass, and the signal becomes rapidly rate-limited. Therefore, we confine ourselves to the signal from third generation squarks with masses around 300–500 GeV, where the signal is likely to be the largest. To unequivocally separate out the third generation signal, we

Table 5 The set of cuts imposed from below that we examined for our study of the extraction of the third generation squark signal at the LHC. Additional cuts were also imposed from above to optimize the third generation squark signal relative to that from the production of heavier gluinos and squarks of the first two generations, as discussed in the text and detailed in Table 6

Variable	Values
$E_T^{\rm miss}$ (GeV) $\geq$	100, 150, 200, 250
$[E_T(j_1), E_T(j_2)]$ (GeV) $\geq$	(100, 100), (200, 100), (200, 150), (300, 100), (300, 150), (300, 200), (400, 100), (400, 150), (400, 200)
$E_T(j_3)$, $E_T(j_4)$ (GeV) $\geq$	100
$E_T(b_1)$ (GeV) $\geq$	40, 100, 200, 300, 400
$m_{\rm eff}$ (GeV) $\geq$	500, 600, ..., 1500
$n_j \geq$	4, 5, 6, 7
$n_b \geq$	1
$S_T \geq$	0.1

must use cuts that are hard enough to reduce the SM backgrounds to acceptable levels, yet not so hard as to enhance the "contamination" from heavier sparticles that, though they are produced with (much) smaller cross sections than third generation squarks, would pass these hard cuts with a much larger efficiency.

Since third generation sfermions decay preferentially to third generation fermions (we focus on the case where $\tilde{t}_1 \to b\widetilde{W}_1$ is accessible), we study the signal with at least one tagged b jet. We found, however, that even the softest set of cuts in Table 2 that we actually use for our analysis of the SUSY b-tagged signal are too hard for the purpose of extracting the signal from third generation squarks. We, therefore, returned to our basic cuts,

$$E_T^{\rm miss} > 100\ {\rm GeV}, \qquad E_T(j_1, j_2) > 100\ {\rm GeV}$$

and augmented these with the requirements

$$E_T(j_3, j_4) > 100\ {\rm GeV}, \qquad S_T \geq 0.1, \qquad n_b \geq 1,$$

and ran the third generation signal through the analysis cuts in Table 5 to extract the optimal $N_{\rm signal}/N_{\rm back}$ ratio (where the background includes the SM and the SUSY contamination as we discussed). These cuts, which are applied "from below", primarily serve to control the SM background which is very large after just the basic cuts (see Table 1) but reduced by the additional requirements of a tagged b jet and two additional 100 GeV jets.

We show the results of our analysis in Table 6. The parameters are shown in the first four rows of the table, while the next few rows show representative sparticle masses. The first two cases are along the $\mu < 0$ model line that we had introduced previously. In the first two cases $B(\tilde{t}_1 \to b\widetilde{W}_1) = 1$, while in Case 3, $B(\tilde{t}_1 \to b\widetilde{W}_1) = 0.74$, with the remainder being made up by the decay $\tilde{t}_1 \to t\widetilde{Z}_1$. The next several rows list the optimized choice of cuts from the $4 \times 9 \times 5 \times 11 \times 4$ possibilities in Table 5, along with the cross sections for (i) the third generation signal, (ii) the SM background, and (iii) the "SUSY contamination" defined as the SUSY sig-

Table 6 Optimized cuts, along with cross sections for the signal from direct production of light third generation squarks, for SM background, and for SUSY contamination to the third generation squark signal. Input parameters and selected sparticle masses are shown in the first ten rows. The next several rows give details on our choice of cuts from the set in Table 5, along with cross sections for the third generation signal, for SUSY contamination, and for the SM background after these cuts. The last six rows show the cut "from above" discussed in the text, along with our final results for the observability of the third generation signal over total backgrounds, including SUSY contamination

	Case 1	Case 2	Case 3
m_{16} (GeV)	717	854	739
$m_{1/2}$ (GeV)	306	355	361
A_0 (GeV)	−1434	−1708	−1478
$\tan\beta$	47	47	47
[3pt] μ (GeV)	−372	−428	−477
$m_{\tilde{g}}$ (GeV)	764	879	886
$m_{\tilde{u}_R}$ (GeV)	966	1127	1070
$m_{\tilde{t}_1}$ (GeV)	274	316	460
$m_{\tilde{b}_1}$ (GeV)	442	559	400
$m_{\widetilde{W}_1}$ (GeV)	236	279	287
[3pt] $E_T^{\rm miss}$ (GeV) >	150	100	150
$[E_T(j_1), E_T(j_2)]$ (GeV) >	(100, 100)	(100, 100)	(200, 100)
$E_T(b_1)$ (GeV) >	40	40	40
$m_{\rm eff}$ (GeV) >	500	500	600
$n_j \geq$	5	6	4
$\sigma_{\rm 3rd\ gen.}$ (fb)	120.2	74.1	80.6
$\sigma_{\rm SUSY\ cont.}$ (fb)	1176.3	590.6	828.9
$\sigma_{\rm SM}$ (fb)	432.6	454.1	580.4
[3pt] $m_{\rm eff}$ (GeV) <	1000	1000	1000
$\sigma_{\rm 3rd\ gen.}$ (fb)	47.2	30.9	20.5
$\sigma_{\rm SUSY\ cont.}$ (fb)	109.5	42.0	40.0
$\sigma_{\rm SM}$ (fb)	141.7	180.6	155.1
$\sigma_{\rm 3rd\ gen.}/\sigma_{\rm tot.\ bkg}$	0.188	0.14	0.105
$N_{\rm signal}/\sqrt{N_{\rm back}}$	29.8	20.7	14.7

nal from production of sparticles other than third generation squarks, after these cuts. We see from these cross sections that both the event rates and the statistical significance of the third generation signal (even with the SUSY contamination included in the background) are very large. The problem, however, is that the signal to background ratio is smaller than 0.1 if the SUSY contamination is included in the background, and it fails to satisfy our observability criterion.[10] We can, however, reduce the SUSY contamination (primarily from heavier sparticles) relative to the third generation signal by requiring that *the signal is not too hard.* Toward this end, we impose an *upper limit*, $m_{\rm eff} < 1000$ GeV, which efficiently reduces the contamination from heavy sparticles with correspondingly modest reduction of the cross sections from the softer third generation and SM processes. The corresponding cross sections after this cut are shown on the next three rows of the table, while the last row shows the final two signal to total background ratios that we are able to obtain, along with the statistical significance of the third generation signal with an integrated luminosity of 100 fb^{-1}.

Several features about the table are worth noting.

- We see from the table that before the cut restricting the value of $m_{\rm eff}$ from above, the background was dominated by SUSY contamination. In contrast, after this cut, the dominant source to the background comes from SM processes.
- With the cuts that we have devised, the event rates for the third generation signal as well as its statistical significance are large. For reasons already discussed, we do not, however, believe that it will be easy to unequivocally ascertain the direct production of third generation squarks in the signal. For this to be unambiguously possible, it will be necessary to have an understanding of the contributions from other SUSY sources to the event rate after our cuts. This may well be possible because with hard cuts it should be possible to isolate the signal from heavy squarks and gluinos where contamination from both SM and the lighter third generation squarks is small. Just how well it will be possible to extrapolate this measured signal into "softer kinematic regions" will determine the precision with which the SUSY contamination can be subtracted. This issue is beyond the scope of the present analysis.
- We examined additional cuts on $E_T(j_1, j_2)$ and n_j to see if we could raise the signal to background ratio. We found that a small increase ($\sim$10%) may indeed be possible by restricting n_j from above to be smaller than 8 or 9. Since our calculation of the background with high jet multiplicity is carried out only in the shower approximation, we did not feel that our estimate of this improvement is reliable and choose not to include it in the table.
- We stress again that the SUSY contamination is model-dependent. We can see from the table that if gluinos and other squarks are indeed decoupled at the LHC, and only third generation squarks are light, their signal should be readily observable in all three cases.

[10] Many authors do not impose such a requirement on the observability of the signal. We believe that some requirement on the $N_{\rm signal}/N_{\rm back}$ ratio is necessary, since otherwise a signal with 5K events above a background of 1M events would be considered significant. This would indeed be the case if the background were known to a very high precision; however, a systematic uncertainty of 0.5% on the background could clearly wipe out the signal, at least if the signal is extracted by subtracting the theoretically calculated background! In the case at hand, where the SUSY model is not a priori known and has to be arrived at using the same data, it is clear that subtraction of the SUSY contamination will suffer from considerable uncertainty until the data and theory both become mature enough for such a subtraction to be carried out. While our criterion requiring $N_{\rm signal}/N_{\rm back} > 0.25$ is admittedly arbitrary, we believe that it is necessary to impose some lower limit on the signal to background ratio for a semi-realistic assessment.

7 Charm jet tagging

Charm jet tagging offers a different possibility for enhancing the SUSY signal, especially in the case where a light top squark dominantly decays via $\tilde{t}_1 \to c\widetilde{Z}_1$. Charm jets may be tagged via the detection of a soft muon within the jet. Muons inside jets also arise from semi-leptonic decays of b-quarks and from accidental overlaps of unrelated muons with jets. Since m_b is significantly larger than m_c, the variables $|\vec{p}_T^{\rm rel}| \equiv |\vec{p}_T(\mu) \times \hat{p}_j|$ and $\Delta R(\mu, j) \equiv \sqrt{\Delta\phi(\mu, j)^2 + \Delta\eta(\mu, j)^2}$ can serve to distinguish muon-tagged c jets from correspondingly tagged b jets or accidental overlap of an unrelated muon with jets. Charm jet tagging with soft muons was first examined in Refs. [126, 127] as a way of enhancing the t-squark signal from $p\bar{p} \to \tilde{t}\tilde{t}X \to cc + E_T^{\rm miss} + X$ production at Run I of the Fermilab Tevatron, but it was found to have a reach smaller than the reach obtained via the conventional $E_T^{\rm miss}$ analysis *because the muon-tagged signal was severely rate-limited*. It was, however, subsequently shown that using soft muons to tag the c jet indeed enhances the top-squark reach [71] but only for an integrated luminosity larger than $\sim$1 fb^{-1}, available today after the upgrade of the Main Injector.

These considerations led us to examine whether charm tagging may be similarly used at the LHC, at least for the case where $\tilde{t} \to c\widetilde{Z}_1$. Since the goal is to separate the charm jets from the decay of $\tilde{t}_1$ from other SUSY sources (which are frequently rich in b jets), it is crucial to be able to separate the c and b jets with at least moderate efficiency and purity. Following Ref. [71], we examined many strategies to obtain this separation in the plane formed by the variables $|\vec{p}_T^{\rm rel}|$ and $\Delta R(\mu, j)$ but without any success. The difference between the situation at the Fermilab Tevatron, where

this strategy appears to be moderately successful, and the LHC is the kinematics of the events. In contrast to the Tevatron, where jets with $E_T > 25$ GeV are readily detectable, at the LHC we have required $E_T(j) > 50$ GeV in order not to be overwhelmed by mini-jet production. For this harder jet kinematics, the difference between m_b and m_c appears to be too small to yield significant separation between c and b jets that are not vertex-tagged. The larger contamination from b jets at the LHC only exacerbates this situation.

Before closing this section, we also mention one other (also unsuccessful) strategy that we tried for c-tagging. The idea was to utilize the difference in the distributions of $z \equiv E_\mu/E_c$ for muons of a fixed sign of the charge from b or $\bar{c}$ decays. While the expected distributions from the quark decays are indeed significantly different, this strategy also fails because these quarks hadronize before they decay, and the z-distributions of the muons from the corresponding bottom or charm meson decays are essentially the same.

8 Summary

The search for gluinos and squarks of supersymmetry is an important item on the agenda of LHC experiments. In most models $m_{\tilde{g}} \lesssim m_{\tilde{q}}$, so that, except when squarks and gluinos are close in mass, we expect squarks to decay mainly to gluinos. The decay patterns of the gluino will then determine the topologies of the bulk of SUSY events at the LHC. Generally speaking, we expect that sparticle production at the LHC will be signaled by an excess of n jet + m isolated leptons + $E_T^{\rm miss}$ events (possibly together with isolated hard photons), with the relative rates for the various topologies determined by the sparticle decay patterns. However, there are a number of well-motivated models (see Sect. 2) in which gluinos preferentially decay to third generation fermions, so that SUSY events are likely to include b or even t jets. Since a large part of the SM background to the inclusive jets + $E_T^{\rm miss}$ SUSY signal comes from $V + E_T^{\rm miss}$ production ($V = W, Z$) and from QCD, b jet tagging should serve to discriminate between the SM and SUSY sources of missing transverse energy events at the LHC. In the HB/FP region of the mSUGRA model favored by the WMAP determination of the relic density, b-tagging increases the LHC reach for gluinos by ∼20% [65, 117] depending on the tagging efficiency and purity that is ultimately attained. Though this does not appear to be a large enhancement, we must remember that we are probing the gluino mass range where the production cross section is already small due to kinematic considerations.

In Sect. 4, we have examined the impact of b-tagging on the LHC reach for a variety of models introduced in Sect. 2. We use a conservative projection for the tagging efficiency of b jets in the high luminosity LHC environment: 50% for central b jets with $E_T \geq 40$ GeV. We find that while b-tagging does indeed increase the SUSY reach of the LHC, the enhancement is typically *smaller* than that found for the HB/FP region of the mSUGRA model. In this model, squarks are in the multi-TeV range; consequently, the SUSY signal (after selection cuts) comes mainly from the pair production of gluinos, whose decays are "b-rich" as we mentioned above. This same enhancement is not obtained in models in which squarks and gluinos have comparable masses. Then, the branching fraction for the decay $\tilde{q} \to q\tilde{g}$ is kinematically suppressed, and the squarks mainly decay via $\tilde{q} \to q\widetilde{Z}_i$ and $\tilde{q} \to q'\widetilde{W}_i$, where the daughter quark (mostly) belongs to the same generation as the parent squark. Since (for values of $m_{\tilde{q}} \gtrsim 1$ TeV) first generation squarks are much more abundantly produced at the LHC than squarks of other generations by the collisions of (first generation) valence quarks in the proton, their decays do not lead to b jets. As a result, (and this is confirmed by our results in Sect. 4) b-tagging enhances the LHC reach the most in models in which squarks are significantly heavier than gluinos: if instead squark production is the origin of a substantial portion of the SUSY $E_T^{\rm miss}$ signal, b-tagging will not be helpful and could even lead to a degradation of the reach of the LHC.

Since the mechanisms that lead to enhanced decays of gluinos to b-quarks mostly revolve around the large third generation Yukawa couplings, these typically also enhance sparticle decays to t-quarks (if these are not kinematically suppressed). This led us to examine in Sect. 5 whether tagging t jets (which potentially reduces SM backgrounds even more efficiently than b jet tagging does) could lead to an increased reach for SUSY. We found, however, that this is not the case, because the top-tagging efficiency is very low. Top-tagging may, however, facilitate the reconstruction of SUSY events in favorable cases [124, 125] and, furthermore, can be used to confirm a SUSY signal first detected in other channels.

There are well-motivated models with an inverted squark mass hierarchy, in which third generation squarks are much lighter than other squarks and gluinos. These models would be strikingly confirmed if signals from the direct production of these relatively light top and sbottom squarks as well as from their production as secondaries from gluino decays could be separately identified. Since the latter possibility has already been studied in Refs. [124, 125], we concentrated on the signal from direct production of third generation squark pairs in Sect. 6. We found that, while these may be readily separated from SM backgrounds, it may be more difficult to discriminate between them and the signal from the production of heavier gluinos and first generation squarks. This is, however, clearly a model-dependent question. It could be that gluinos and first generation squarks are so heavy that the SUSY contamination is not an issue at all. Alternatively, if gluinos and first generation squarks are not extremely heavy,

it may be possible to determine their properties by studying the event sample with very hard cuts to remove contributions from the production of the much lighter third generation squarks; we can then use these to subtract the contamination from gluino and first generation squark production in the analysis of the signal from the direct production of third generation squarks.

Finally, in Sect. 7 we have examined whether charm tagging (using muons inside a jet) may be useful to enhance the SUSY signal at the LHC. Our conclusions are pessimistic. The kinematics of events at the LHC (in contrast to the kinematics at the Fermilab Tevatron) makes it very difficult to distinguish between b jets and c jets using the soft-muon-tagging technique.

In summary, we have found that the use of b-tagging enhances the SUSY reach of the LHC by up to 20% in a variety of well-motivated models, with the largest increase in reach being obtained in models with $m_{\tilde{q}} \gg m_{\tilde{g}}$, and no increase (or even a reduction in reach) if squark production is an important part of the signal after the final cuts. For many models, but not all, tagging b- and t-quark jets improves the signal to background ratio, resulting in a cleaner SUSY event sample, which can then be used either to reconstruct SUSY event chains [124, 125] or, as has recently been suggested, possibly to determine the gluino mass [128].[11] In contrast, we find that charm-jet tagging does not appear to be useful at the LHC.

Acknowledgements This research was supported in part by a grant from the United States Department of Energy and by Fundação de Amparo à Pesquisa do Estado de São Paulo (FAPESP). J.K. Mizukoshi would like to thank Instituto de Física da Universidade de São Paulo for the use of its facility.

References

1. H. Baer, X. Tata, *Weak Scale Supersymmetry* (Cambridge University Press, London, 2006)
2. M. Drees, R. Godbole, P. Roy, *Theory and Phenomenology of Sparticles* (World Scientific, London, 2004)
3. P. Binetruy, *Supersymmetry* (Oxford University Press, London, 2006)
4. S. Martin, arXiv:hep-ph/9709356 (1997)
5. H. Baer, C.H. Chen, F. Paige, X. Tata, Phys. Rev. D **52**, 2746 (1995)
6. H. Baer, C.H. Chen, F. Paige, X. Tata, Phys. Rev. D **53**, 6241 (1996)
7. H. Baer, C.H. Chen, M. Drees, F. Paige, X. Tata, Phys. Rev. D **59**, 055014 (1999)
8. ATLAS Collaboration, Technical Design Report, CERN LHCC/99-15 (1999)
9. CMS Collaboration, S. Abdullin et al., arXiv:hep-ph/9806366 (1998)
10. S. Abdullin, F. Charles, Nucl. Phys. B **547**, 60 (1999)
11. G. Bayatian et al., CMS Physics Technical Design Report, vol. II, CERN/LHCC 2006-021 (2006)
12. B. Allanach, J. Hetherington, A. Parker, B. Webber, J. High Energy Phys. **08**, 017 (2000)
13. H. Baer, C. Balazs, A. Belyaev, T. Krupovnickas, X. Tata, J. High Energy Phys. **0306**, 054 (2003)
14. WMAP Collaboration, D.N. Spergel et al., Astrophys. J. Suppl. **170**, 377 (2007)
15. Joint LEP2 Supersymmetry Working Group, ALEPH, DELPHI, L3 and OPAL Collaborations, *Combined Results up to 208 GeV*. http://lepsusy.web.cern.ch/lepsusy/
16. K. Griest, D. Seckel, Phys. Rev. D **43**, 3191 (1991)
17. J. McDonald, K. Olive, M. Srednicki, Phys. Lett. B **283**, 80 (1992)
18. S. Mizuta, M. Yamaguchi, Phys. Lett. B **298**, 120 (1993)
19. J. Ellis, T. Falk, K. Olive, Phys. Lett. B **444**, 367 (1998)
20. J. Ellis, T. Falk, K. Olive, M. Srednicki, Astropart. Phys. **13**, 181 (2000)
21. M.E. Gómez, G. Lazarides, C. Pallis, Phys. Rev. D **61**, 123512 (2000)
22. M.E. Gómez, G. Lazarides, C. Pallis, Phys. Lett. B **487**, 313 (2000)
23. A. Lahanas, D.V. Nanopoulos, V. Spanos, Phys. Rev. D **62**, 023515 (2000)
24. R. Arnowitt, B. Dutta, Y. Santoso, Nucl. Phys. B **606**, 59 (2001)
25. C. Böhm, A. Djouadi, M. Drees, Phys. Rev. D **30**, 035012 (2000)
26. J.R. Ellis, K.A. Olive, Y. Santoso, Astropart. Phys. **18**, 395 (2003)
27. J. Edsjö et al., J. Cosmol. Astropart. Phys. **0304**, 001 (2003)
28. M. Drees, M. Nojiri, Phys. Rev. D **47**, 376 (1993)
29. H. Baer, M. Brhlik, Phys. Rev. D **53**, 597 (1996)
30. H. Baer, M. Brhlik, Phys. Rev. D **57**, 567 (1998)
31. H. Baer, M. Brhlik, M. Diaz, J. Ferrandis, P. Mercadante, P. Quintana, X. Tata, Phys. Rev. D **63**, 015007 (2001)
32. J. Ellis, T. Falk, G. Ganis, K. Olive, M. Srednicki, Phys. Lett. B **510**, 236 (2001)
33. L. Roszkowski, R. Ruiz de Austri, T. Nihei, J. High Energy Phys. **0108**, 024 (2001)
34. A. Djouadi, M. Drees, J.L. Kneur, J. High Energy Phys. **0108**, 055 (2001)
35. A. Lahanas, V. Spanos, Eur. Phys. J. C **23**, 185 (2002)
36. V. Berezinski et al., Astropart. Phys. **5**, 1 (1996)
37. V. Berezinski et al., Astropart. Phys. **5**, 333 (1996)
38. P. Nath, R. Arnowitt, Phys. Rev. D **56**, 2820 (1997)
39. A. Bottino, F. Donato, N. Fornengo, S. Scopel, Phys. Rev. D **59**, 095004 (1999)
40. A. Bottino, F. Donato, N. Fornengo, S. Scopel, Phys. Rev. D **63**, 125003 (2001)
41. J. Ellis, K. Olive, Y. Santoso, Phys. Lett. B **539**, 107 (2002)
42. J. Ellis, T. Falk, K. Olive, Y. Santoso, Nucl. Phys. B **652**, 259 (2003)
43. M. Drees, hep-ph/0410113
44. H. Baer, A. Mustafayev, S. Profumo, A. Belyaev, X. Tata, Phys. Rev. D **71**, 095008 (2005)
45. H. Baer, A. Mustafayev, S. Profumo, A. Belyaev, X. Tata, J. High Energy Phys. **0507**, 065 (2005)
46. R. Arnowitt, P. Nath, Phys. Rev. Lett. **70**, 3696 (1993)
47. A. Djouadi, M. Drees, J. Kneur, Phys. Lett. B **624**, 60 (2005)
48. S. Martin, Phys. Rev. D **75**, 115005 (2007)
49. S. Martin, Phys. Rev. D **75**, 095005 (2007)
50. H. Baer, A. Box, E.K. Park, X. Tata, J. High Energy Phys. **0708**, 060 (2007)
51. K.L. Chan, U. Chattopadhyay, P. Nath, Phys. Rev. D **58**, 096004 (1998)
52. J. Feng, K. Matchev, T. Moroi, Phys. Rev. Lett. **84**, 2322 (2000)

[11] The technique suggested here depends crucially on the ability to reliably calculate the absolute cross section of the SUSY signal after hard cuts and background subtraction.

53. J. Feng, K. Matchev, T. Moroi, Phys. Rev. D **61**, 075005 (2000)
54. G. Belanger et al., Nucl. Phys. **706**, 411 (2005)
55. Y. Mambrini, E. Nezri, Eur. Phys. J. C **50**, 949 (2007)
56. H. Baer, A. Mustafayev, E.K. Park, S. Profumo, X. Tata, J. High Energy Phys. **0604**, 041 (2006)
57. H. Baer, A. Mustafayev, S. Profumo, X. Tata, Phys. Rev. D **75**, 035004 (2007)
58. H. Baer, A. Mustafayev, H. Summy, X. Tata, J. High Energy Phys. **0710**, 088 (2007)
59. A. Birkedal-Hansen, B. Nelson, Phys. Rev. D **64**, 015008 (2001)
60. A. Birkedal-Hansen, B. Nelson, Phys. Rev. D **67**, 095006 (2003)
61. H. Baer, A. Mustafayev, E.K. Park, S. Profumo, J. High Energy Phys. **0507**, 046 (2005)
62. H. Baer, T. Krupovnickas, A. Mustafayev, E.K. Park, S. Profumo, X. Tata, J. High Energy Phys. **0512**, 011 (2005)
63. H. Baer, A. Mustafayev, E.K. Park, X. Tata, J. High Energy Phys. **0805**, 058 (2008)
64. U. Chattopadhyay, A. Datta, A. Datta, A. Datta, D.P. Roy, Phys. Lett. B **493**, 127 (2000)
65. P.G. Mercadante, J.K. Mizukoshi, X. Tata, Phys. Rev. D **72**, 035009 (2005)
66. J. Feng, C. Kolda, N. Polonsky, Nucl. Phys. B **546**, 3 (1999)
67. J. Bagger, J. Feng, N. Polonsky, Nucl. Phys. B **563**, 3 (1999)
68. J. Bagger, J. Feng, N. Polonsky, R. Zhang, Phys. Lett. B **473**, 264 (2000)
69. H. Baer, P. Mercadante, X. Tata, Phys. Lett. B **475**, 289 (2000)
70. H. Baer et al., Phys. Rev. D **64**, 015002 (2001)
71. J. Sender, PhD thesis. hep-ph/0010025
72. F. Paige, S. Protopopescu, H. Baer, X. Tata, hep-ph/0312045
73. A. Chamseddine, R. Arnowitt, P. Nath, Phys. Rev. Lett. **49**, 970 (1982)
74. R. Barbieri, S. Ferrara, C. Savoy, Phys. Lett. B **119**, 343 (1982)
75. N. Ohta, Prog. Theor. Phys. **70**, 542 (1983)
76. L.J. Hall, J. Lykken, S. Weinberg, Phys. Rev. D **27**, 2359 (1983)
77. H.P. Nilles, Phys. Rep. **110**, 1 (1984)
78. P. Nath, hep-ph/0307123
79. L.E. Ibañez, G.G. Ross, Phys. Lett. B **110**, 215 (1982)
80. L. Ibañez, Phys. Lett. B **118**, 73 (1982)
81. J. Ellis, D.V. Nanopoulos, K. Tamvakis, Phys. Lett. B **121**, 123 (1983)
82. L. Alvarez-Gaume, J. Polchinski, M.B. Wise, Nucl. Phys. B **221**, 495 (1983)
83. K. Inoue, A. Kakuto, H. Komatsu, S. Takeshita, Prog. Theor. Phys. **68**, 927 (1982)
84. K. Inoue, A. Kakuto, H. Komatsu, S. Takeshita, Prog. Theor. Phys. **71**, 413 (1984)
85. K. Inoue, A. Kakuto, S. Takeshita, Prog. Theor. Phys. **71**, 348 (1984)
86. J. Feng, K. Matchev, F. Wilczek, Phys. Lett. B **482**, 388 (2000)
87. J. Feng, K. Matchev, F. Wilczek, Phys. Rev. D **63**, 045024 (2001)
88. H. Baer, T. Krupovnickas, S. Profumo, P. Ullio, J. High Energy Phys. **0510**, 020 (2005)
89. Y. Fukuda et al., Phys. Rev. Lett. **82**, 2644 (1999)
90. Y. Fukuda et al., Phys. Rev. Lett. **85**, 3999 (1999)
91. Q.R. Ahmad et al., Phys. Rev. Lett. **89**, 011301 (2002)
92. K. Eguchi et al., Phys. Rev. Lett. **90**, 021802 (2003)
93. T. Araki et al., Phys. Rev. Lett. **94**, 081801 (2005)
94. S. Abe et al., arXiv:0801.4589 [hep-ex], for visual evidence of neutrino oscillation
95. H. Georgi, in *AIP Proceedings*, ed. by C. Carlson (1974)
96. H. Fritzsch, P. Minkowski, Ann. Phys. **93**, 193 (1975)
97. M. Gell-Mann, P. Ramond, R. Slansky, Rev. Mod. Phys. **50**, 221 (1978)
98. R. Mohapatra, hep-ph/9911272, for a pedagogical review
99. M. Drees, Phys. Lett. B **181**, 279 (1986)
100. J.S. Hagelin, S. Kelley, Nucl. Phys. B **342**, 95 (1990)
101. A.E. Faraggi et al., Phys. Rev. D **45**, 3272 (1992)
102. Y. Kawamura, M. Tanaka, Prog. Theor. Phys. **91**, 949 (1994)
103. Y. Kawamura et al., Phys. Lett. B **324**, 52 (1994)
104. Y. Kawamura et al., Phys. Rev. D **51**, 1337 (1995)
105. N. Polonsky, A. Pomarol, Phys. Rev. D **51**, 6532 (1994)
106. H.-C. Cheng, L.J. Hall, Phys. Rev. D **51**, 5289 (1995)
107. C. Kolda, S.P. Martin, Phys. Rev. D **53**, 3871 (1996)
108. R. Dermisek, S. Raby, Phys. Rev. D **62**, 015007 (2000)
109. T. Blazek, R. Dermisek, S. Raby, Phys. Rev. D **65**, 115004 (2002)
110. R. Dermisek, S. Raby, L. Roszkowski, R. Ruiz de Austri, J. High Energy Phys. **0509**, 029 (2005)
111. R. Dermisek, M. Harada, S. Raby, Phys. Rev. D **74**, 035011 (2006), and references therein
112. H. Baer, M. Díaz, J. Ferrandis, X. Tata, Phys. Rev. D **61**, 111701 (2000)
113. D. Auto, H. Baer, C. Balazs, A. Belyaev, J. Ferrandis, X. Tata, J. High Energy Phys. **0306**, 023 (2003)
114. H. Baer, S. Kraml, S. Sekmen, H. Summy, J. High Energy Phys. **0803**, 056 (2008)
115. M. Albrecht, W. Altmannshofer, A. Buras, D. Guadagnoli, D. Straub, J. High Energy Phys. **0710**, 055 (2007)
116. W. Altmannshofer, D. Guadagnoli, S. Raby, D. Straub, arXiv:0801.4363 [hep-ph]
117. S.P. Das, A. Datta, M. Guchait, M. Maity, S. Mukherjee, Eur. Phys. J. C **54**, 645 (2008)
118. S. Corréad, V. Kostioukhine, J. Levêque, A. Rozanov, J.B. de Vivie, ATLAS Note, ATLAS-PHYS-2004-006
119. V. Kostioukhine, ATLAS Note, ATLAS-PHYS-2003-033
120. H. Baer, J. Ellis, G. Gelmini, D.V. Nanopoulos, X. Tata, Phys. Lett. B **161**, 175 (1985)
121. G. Gamberini, Z. Phys. C **30**, 605 (1986)
122. H. Baer, V. Barger, D. Karatas, X. Tata, Phys. Rev. D **36**, 96 (1987)
123. H. Baer, X. Tata, J. Woodside, Phys. Rev. D **45**, 142 (1992)
124. J. Hisano, K. Kawagoe, M. Nojiri, Phys. Rev. D **68**, 035007 (2003)
125. J. Hisano, K. Kawagoe, R. Kitano, M. Nojiri, Phys. Rev. D **66**, 115004 (2002)
126. H. Baer, J. Sender, X. Tata, Phys. Rev. D **50**, 4517 (1994)
127. R. Demina, J. Lykken, K. Matchev, A. Nomerotski, Phys. Rev. D **62**, 035011 (2000)
128. H. Baer, V. Barger, G. Shaughnessy, H. Summy, L.-T. Wang, Phys. Rev. D **75**, 095010 (2007)